1
Dimensions and Surfaces – an Introduction

This first chapter can be seen as a warm-up: it will prepare our mental muscles to think about nanomaterials, and why they can be considered as a class of materials in their own right. We will introduce the concept of confinement and dimensionality and derive the density of states (DOS) for low-dimensional structures. After a discussion of electronic properties we will move on to a quite different area of research, and discuss fundamental processes at surfaces, which are rarely included in materials science or physics core classes, but are important for the understanding of many aspects of nanomaterial synthesis.

1.1
Size, Dimensionality, and Confinement

The nanosize regime is defined by the transition between the bulk and atom, and is characterized by a rapid change in material properties with size. Each set of properties (mechanical properties, geometric and electronic structure, magnetic and optical properties, and reactivity) is defined by characteristic length scales. If the size of the system approaches a characteristic length scale, the property in question will be modified dramatically as a function of size. The intimate link between size and material properties is one of the most intriguing aspects of nanoscience, and is at the core of the discipline. The control of size is therefore often the most important, and difficult, challenge in the synthesis of nanostructures.

The decrease in size of a nanostructure is accompanied by a rapid change in the volume-to-surface ratio of atoms: a cube with a side length of 1 mm contains about $2.5 \cdot 10^{19}$ atoms, and the percentage of surface atoms is only $2 \cdot 10^{-6}$; for a cube side length of 1 μm the percentage of surface atoms increases to $2 \cdot 10^{-3}$; and for 1 nm side length, only one true volume atom remains, which is surrounded on all sides by other atoms. This shift from a volume–atom dominated structure, where the majority of atoms has fully

Inorganic Nanostructures: Properties and Characterization, First Edition. Reinke, P.

Published 2012 by WILEY-VCH Verlag GmbH & Co. KGaA

saturated bonds, to a surface–atom dominated structure has rather dramatic consequences.

One of the best-known examples, which illustrates the impact of the change in the ratio of surface-to-volume atoms, is the observation of the reactivity of nanosize catalyst particles [1–3]. Catalysts are industrial materials, which are produced in very high volumes and used in nearly every chemical process. The role of a catalyst in a chemical reaction is to lower the activation energies in one or several of the reaction steps, and it can therefore increase yield, reaction speed, and selectivity. Most catalysts contain a relatively high percentage of expensive noble metals, and increasing catalyst efficiency through reduction of its size can thus greatly diminish costs, and at the same time very often boosts efficiency. The reactivity increase with decreasing particle size can be attributed to several size dependent factors: a proportional increase in the number of reactive surface atoms and sites, changes in the electronic structure, and differences in the geometric structure and curvature of the surface, which presents a larger concentration of highly active edge and kink sites. The underlying mechanism of a catalytic reaction is often complex, and cannot be attributed to a single factor such as larger surface area or modulation of the electronic structure. The study of catalysts and catalytic reactions is a highly active field of research, and depends on the improved comprehension of nanoparticle synthesis and properties.

An important step in classifying the functionality of nanostructures is to understand the relation between dimensionality and confinement. Dimensionality is mathematically defined by the minimum number of coordinates required to define each point within a unit; this is equivalent to vectors which define a set of n unit vectors required to reach each point within an n-dimensional space. When looking at nanostructures, the definition of dimensionality becomes more ambiguous: for example, a semiconductor nanowire can have a diameter of a few to several ten nanometers, with a length up to several micrometers. It is a structure with a very high aspect ratio, but in order to describe the position of each atom or unit cell within the wire, a three-dimensional (3D) coordinate system is required with one axis along the wire and the other two unit vectors to describe the position within the horizontal plane. This coordinate system bears no relation to the crystal structure and only serves to illustrate the mathematical dimension of the nanowire. A one-dimensional (1D) nanowire is therefore strictly speaking only present if its thickness is only a single atom. Examples for this kind of 1D system are given in Chapter 3.

The most important aspect for our discussion of dimensionality is the modulation of the electronic structure as a function of the extension of a nanostructure in the three dimensions of space. It is possible to define potential barriers in a single direction in space, thus confining electrons in one direction, but leaving them unperturbed in the other two directions. This corresponds now to a two-dimensional (2D) nanostructure, a so-called quantum well. Going back to our example of the nanowire: the electronic system of the nanowire (if it is sufficiently small) is confined in the two directions perpendicular to its long axis, but not along the long axis itself, and it is therefore a 1D structure. The dimensionality of a nanostructure is defined through the geometry of the confinement potential.

Dimensionality for nanostructures is therefore often defined in a physically meaningful manner by considering the directions of electron confinement. Confinement for electrons is introduced in quantum mechanics by using the particle in a box: the electron wave is confined within the well, which is defined by infinitely high potential energy barriers. The equivalent treatment can be used for holes. The width of the box then controls the energy spacing between the allowed states, which are obtained from solutions of the Schrödinger equation.

The allowed n-th energy level E_n is given for a 1D well (a one dimensional box, with only one directional axis) by:

$$E_n = \frac{\hbar^2 n^2 \pi^2}{L^2 2m^*} = \frac{h^2 n^2}{8m^* L^2} \tag{1.1}$$

where L is the width of the box, m^* is the effective mass of the electron, and n is an integer 1, 2, 3, ... This equation emerges directly from the solution of the Schrödinger equation for the free electrons in a 1D box with a width of L, which is described in quantum mechanics textbooks. The energy increases with the inverse of the square of the box size, and n is the corresponding quantum number. This relation is quite general, and specific factors and exponents are modified by the shape of the confinement potential. The highest filled level at a temperature of 0 K corresponds to the Fermi energy (E_F) and the quantum well is in its ground state when all levels up to E_F are filled. The band gap is the energy difference between the ground state and the first excited state when one electron is excited to the first empty state above E_F. If we build a very large quantum well whose dimension approaches that of a macroscopic solid, the energy difference between the ground state and excited state will become infinitesimally small compared with the thermal energy, and the band gap created by quantum confinement for small L disappears; we now have a quasi-continuum of states. The height of the well barrier for a solid is given by the work function of the limiting surfaces.

The band gap in a macroscopic solid forms due to the periodicity of the lattice, which imposes boundary conditions on the electron waves and leads for certain energies to standing waves within the lattice. The standing waves whose wavelengths correspond to multiples of interatomic distances in a given lattice direction define the band gap within the band structure ($E(\vec{k})$) of the material (we are neglecting any structure factors on this discussion). The ion cores define the position of the nodes, and extrema of a standing wave. If the wave vector $\vec{k}$ satisfies the Laue diffraction condition within the reciprocal lattice, we will observe opening of a band gap at this specific value of $\vec{k}$, which is the Brillouin zone boundary. The energy gap opens due to the energetic difference between a wave where the nodes are positioned at the ion cores, and a wave of the same wavelength (wave vector) but where the nodes are positioned in between the ion cores. This argument follows the so-called Ziman model and is described in detail in many textbooks on solid state physics. A semicondcutor or insulator results if the Fermi energy E_F is positioned within this bandgap, in all other cases when E_F is positioned in the continuum of states, we will have a metal.

If we now start with a metal, where E_F lies within the continuum of states, and reduce the size of the system to the nanoscale, which is equivalent to the reduction in the size of the box or quantum well L, the energy difference between states will increase and we can open a band gap for sufficiently small dimensions. The macroscopic metal can become a nanoscopic insulator. For a semiconductor, where a fundamental gap is already present, the magnitude of the gap will increase as confinement drives the increase in separation of the energy levels. The measurement of the magnitude of the band gap is therefore a sensitive measure for quantum confinement and is used in all chapters to illustrate and ascertain the presence of confinement.

In the case of a 2D quantum well, if we define the confinement potential along the z axis, the band structure in x, and y will not be perturbed by confinement. Figure 1.1 shows the energy levels in the quantum well in the direction of confinement, z, and illustrates the sub-band formation. The confinement as described in Equation 1.1 only affects the energy levels in the z direction, while the continuum of levels in the x, and y directions is preserved and for the free electron case the dispersion relation is described by a parabola. Each discrete energy level (set of quantum numbers) in the directions of confinement is associated with the energy levels in the other directions; this leads to the formation of sub-bands. This train of thought can be transferred directly to quantum wires, where confinement is in two directions, and quantum dots, where confinement is in all three directions of space and we have a zero-dimensional (0D) electronic structure. Confinement and formation of sub-bands can substantially change the overall band structure, which is discussed for Si nanowires in the context of the blue shift of emission for porous silicon and a transition from an indirect to direct band gap material for small wire diameters [4–6] (see Chapter 4). The size of the gap is a signature of the impact of confinement, and its increase for decreasing size of a nanostructure is illustrated for several types of materials throughout this book. Silicon nanowires and graphene nanoribbons are examples where the increase in the gap was observed experimentally as a function of size.

The confinement potential will only affect the electronic structure if the dimensions of the potential well are in the range or smaller than the de Broglie wavelength, λ, which is given by:

$$\lambda = \frac{h}{(2m^{*}E)^{1/2}} \tag{1.2}$$

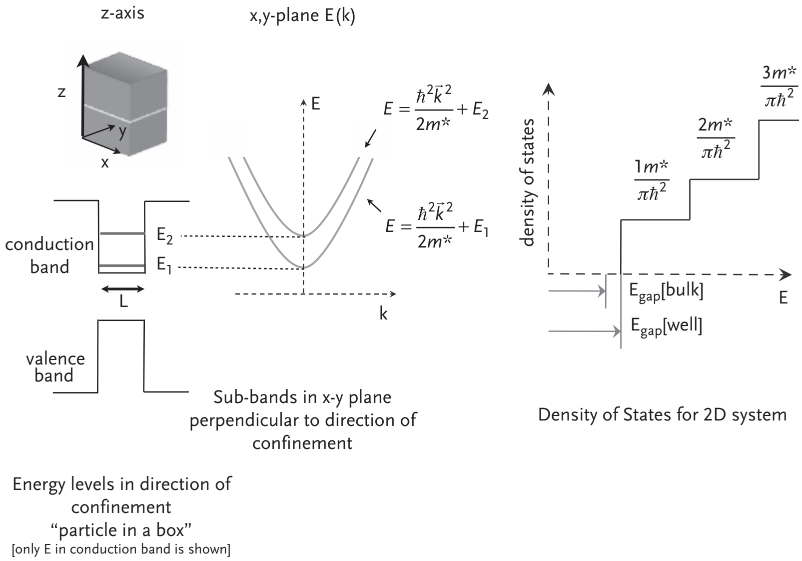

Figure 1.1 The discussion of confinement for a 2D quantum well with one direction of confinement (z axis) is summarized. The QW is sketched on the left hand side: a material with a smaller band-gap (light stripe) is embedded in a material with a larger band-gap (grey). The left-hand figure shows the energy levels within the quantum well, for clarity of illustration only two energy levels are included in the conduction band. The figure in the center shows the two parabolic sub-bands and the total energy of the electrons in these sub-bands, which is composed of the parabolic and the quantized contribution in the z direction. The schematic on the right-hand side shows the corresponding density of states of the conduction band for a 2D quantum well. The band gaps of the bulk material and the quantum well are indicated in this figure: because of the quantification of energy levels due to confinement, the lowest energy level in the conduction band is energetically "higher" than the conduction band minimum in the bulk material, hence the bandgap of the well is larger. The DOS is derived in the text and summarized in Equation 1.7.

where m^* is the electron effective mass, and E is the energy. The de Broglie wavelength of the typical charge carrier for metals is usually only a few nanometers; the values for semiconductors are considerably larger, for example GaAs has a de Broglie wavelength of 24 nm[1], while Si has a smaller de Broglie wavelength of around 12 nm. Therefore a metal cluster, as discussed in Chapter 4, will only show confinement effects for very small nanometer-sized clusters, while quantum dots made of semiconductor materials can be an order of magnitude larger and will still exhibit the characteristic 0D DOS with discrete energy levels as a signature of effective confinement.

The experimental challenge now lies in the creation of specific confinement potentials, which provide one-, two-, and three-dimensional

---

[1] http://www.ioffe.ru/SVA/NSM/ is a database of essential semiconductor properties and bandstructures. The de Broglie wavelengths of several semiconductors are included here: http://www.ioffe.ru/SVA/NSM/Semicond/index.html.

confinement. In reality the height of the confining barrier is not infinite and usually reaches a few tenth to several electron volts at the most. The height of the barrier defines firstly, the temperature, at which charge begins to escape the well due to thermal excitation, and, secondly, the barrier height and distance between adjacent wells determines the tunneling probability and thus charge exchange through extended structures. This becomes important when we build superlattices where the interaction between nanostructures becomes a component of the overall functionality. A confinement potential can be created by interfacing heterostructures with dissimilar band gaps, which can be designed to trap electrons or holes within the well, or we can use the surface, the interface between solid and vacuum [7].

A beautiful example of electron confinement is the so-called quantum corral, where Crommie *et al.* [8, 9] showed for the first time the "image" of an electron wave or more precisely, the spatial variation of the DOS of a standing electron wave in a spherical, planar confinement potential. The quantum corral, which is shown in Figure 1.2 was built from 48 Fe atoms, which form a circle. The atoms are positioned by moving them with the tip in a scanning tunneling microscope, and the sample temperature is sufficiently low to minimize thermal motion of Fe ad-atoms. The electron wave is triggered by injection of an electron at the center of the quantum corral, and is confined by the "wall" of Fe atoms. Confinement is not

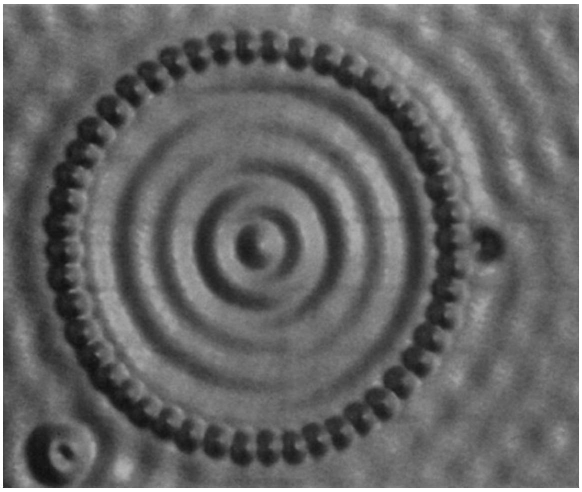

Figure 1.2 Quantum corral [22] of 48 Fe atoms on Cu(111). The Fe atoms are moved into position by the STM tip, which also serves to image the standing electron wave within the corral. The Fe-atom corral acts as confinement potential and the wavelength of electron wave agrees with the solutions of the Schrödinger equation for a planar system. From [22]. Reprinted with permission from AAAS. The individual steps in the quantum corral assembly are shown in some more detail at http://www.almaden.ibm.com/vis/stm/corral.html.

complete, and some small amount of charge leaks out of the corral, which can be seen in the image as a rapidly decaying wave on the outside of the corral. However, the standing wave inside the corral is truly two-dimensional: it is not only confined by the corral but also confined to the surface of the Cu crystal. This appears somewhat counterintuitive since Cu is a metal, but the Cu bulk band structure has a band gap in the (111) direction. The d-band of Cu is positioned a few eV below the Fermi energy, and the sp-band crosses the Fermi energy in the (110) and the (100), but not in the (111) direction [10]. The 3D band structure of Cu therefore has no electronic states in this direction, but the 2D band structure of the Cu(111) surface presents so-called surface states, which can be calculated from the solution of the Schrödinger equation for the 2D surface lattice. The band gap in the bulk, 3D band structure confines this 2D state to the surface, and prevents propagation of the electron wave into the bulk. The confinement of the surface state, and the confinement by the artificial corral made of Fe atoms are required to produce the beautiful standing wave, which can then be imaged with scanning tunneling microscopy (STM).

1.1.1
Density of States for 3,2,1,0 Dimensions

The reduction of dimensionality changes the electronic structure decisively and we derive here the density of states (DOS) for the 3D to 0D case. The DOS $\mathrm{d}N/\mathrm{d}E \cdot 1/V$ of an electronic system is defined as the number of electronic states $\mathrm{d}N$, which occupy a given energy interval $\mathrm{d}E$ per unit volume (V). The DOS for electrons within a 3D solid can be derived as following, starting from the expression for the energy E_n of a state within the solid as a function of the wave vector k. The electrons are in this case treated as free electrons, and the spatial variation in the Coulomb interaction with the ion cores is neglected. The energy is given for the 3D case in analogy to Equation 1.1 by:

$$E_n = \frac{\hbar^2 \vec{k}^2}{2m^*} = \frac{\hbar^2}{2m^*}(k_x^2 + k_y^2 + k_z^2) = \frac{2\pi^2\hbar^2}{L^2 m^*}(n_x^2 + n_y^2 + n_z^2) \qquad (1.3)$$

with the wave vector component $k = 2\pi n/L$ (each wave vector is described here as a cube whose position in space is determined by the associated quantum numbers, whereas L is the side length of a cube of solid material). n_x, n_y, and n_z are the quantum numbers which characterize each individual energy state, which can be occupied by two electrons of opposite spin. We now use a geometrical description of the space of quantum numbers, and redefine n_x, n_y, and n_z as a position vector (n_x, n_y, n_z). The endpoint of each of these vectors is a unique position in space, which corresponds to exactly one energy state and a primitive unit cell, which can hold two electrons of opposite spin. The volume of an allowed state in k space is then given by $(2\pi/L)^3$. The highest occupied energy state at 0 K is the Fermi energy, which corresponds in this geometric picture to a sphere. The DOS is obtained by dividing the volume of a spherical shell (which corresponds to an energy interval) by the volume of a single state. The volume of the spherical shell from radius $\vec{k}$ to $\vec{k} + d\vec{k}$ is given by:

$$V_{shell}\mathrm{d}\vec{k} = 4\pi|\vec{k}^2|\mathrm{d}\vec{k} \tag{1.4}$$

and is then divided by the volume of the single state, which yields the number of states in this shell:

$$\frac{\mathrm{d}N}{\mathrm{d}\vec{k}} = \frac{L^3|\vec{k}^2|}{\pi^2} \tag{1.5}$$

Using the relation between energy and k vector introduced in Equation 1.3, we obtain $\mathrm{d}E/\mathrm{d}k$ and can now determine the number of states per energy interval for a 3D system of free electrons:

$$\mathrm{DOS}_{3\mathrm{D}} = \frac{\mathrm{d}N_{3\mathrm{D}}}{\mathrm{d}E} - \frac{1}{L^3} = \frac{1}{2\pi}\left(\frac{2m^*}{\hbar^2}\right)^{3/2} E^{1/2} \tag{1.6}$$

The expressions for the ideal 2D and 1D systems can be derived in the same way as for the 3D case, and Figure 1.3 schematically shows the DOS for 3D to 0D systems. For the 2D system (e.g., a quantum well) one component in k space is fixed; for the 1D system (e.g., a nanowire) two components in k space are fixed. In the 2D system each state occupies an area of $(2\pi/L)^2$, and in the 1D system this is reduced to a length of $(2\pi/L)$. The derivation of the DOS for the 2D and 1D system is then made in analogy to the 3D case, using the area of an annulus (2D) and the length of line segment (1D), respectively.

The $\mathrm{DOS}_{2\mathrm{D}}$ is independent of the energy, and becomes a step function:

$$\mathrm{DOS}_{2\mathrm{D}} = \frac{m^*}{\pi\hbar^2} \tag{1.7}$$

And the DOS for the 1D system:

$$\mathrm{DOS}_{1\mathrm{D}} = \frac{1}{\pi}\left(\frac{2m}{\hbar^2}\right)^{1/2} \frac{1}{E^{1/2}} \tag{1.8}$$

The DOS, which are derived here, are the solutions for the ideal system, for example, a 2D sheet without any contributions from a third direction. For a 0D system such as a quantum dot, the energy levels become fully discrete, and the DOS shows only discrete lines, which correspond to the

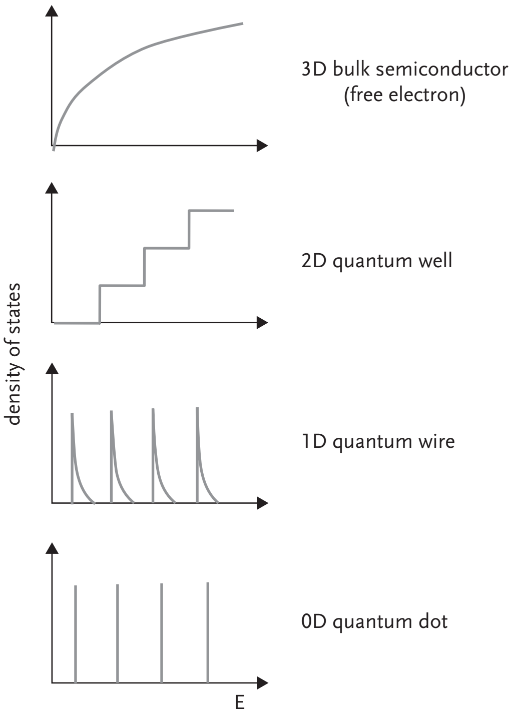

Figure 1.3 Schematic illustration of the density of states for 3D to 0D systems.

atom-like discrete spectrum. Semiconductor quantum dots or ultrasmall metal clusters are therefore often labeled as “artificial atoms”.

1.2
Synthesis of Nanostructures: Fundamental Surface Processes and Reactions

The rapid change in properties and stability as a function of size and dimensionality places rather stringent conditions on the synthesis of nanostructures. A multitude of different methods has been developed, and we often distinguish between top-down and bottom-up approaches. Lithography-based techniques, which are essential in semiconductor device fabrication, are top-down techniques, where an artificial structure is constructed by sequential deposition and etching steps. The length scale is defined and limited by the wavelength and energy of the electron, ion, or photon beam, which is used to write the respective structural features.

In a bottom-up approach the nanostructure is essentially assembled from the smallest unit, often aided by the use of a template or a self-assembly process. This approach allows access to the size regime below 10 nm, which can currently not be reached by lithography. The methods used for the synthesis of the basic nanoscale units, such as the semiconductor nanowires, carbon nanotubes, or quantum dots, are highly diverse and are discussed in detail in the chapters devoted to these groups of materials. In this introductory chapter we will provide the reader with a basic understanding of the fundamental surface processes and reactions.

The importance of fundamental surface processes for controlling shape, structure, and composition was recognized early on in systematic studies of crystal growth. Understanding the interplay between surface reactions has become even more critical in order to achieve control of nanostructure synthesis and to reach at least some degree of predictability in designing new nano-sized building blocks and arrays of building blocks. The fundamental surface processes can be subdivided into four groups, as shown schematically in Figure 1.4: (i) adsorption and desorption, (ii) diffusion, (iii) nucleation, and (iv) growth. While all of these processes are intimately linked, it is helpful to discuss them separately, at least in the beginning.

However, before we start to discuss the fundamental surface processes we must take a closer look at the electronic and geometric structure of a surface. In the so-called terrace-step-kink (TSK) model each atom is represented by a single cube. This representation of the surface was also chosen in Figure 1.5. The TSK model helps to recognize different geometric defects on the surface, such as step edges, point defects, and kink sites, which are under-coordinated lattice atoms and thus often serve as preferential reaction or nucleation sites. The TSK model, however, fails to represent the geometric structure on the atomic scale. If a solid is cleaved along a certain lattice plane, the atoms, which are now positioned on the new surface, experience a dramatically different bonding environment, and consequently a reorganization of the geometric structure is often necessary

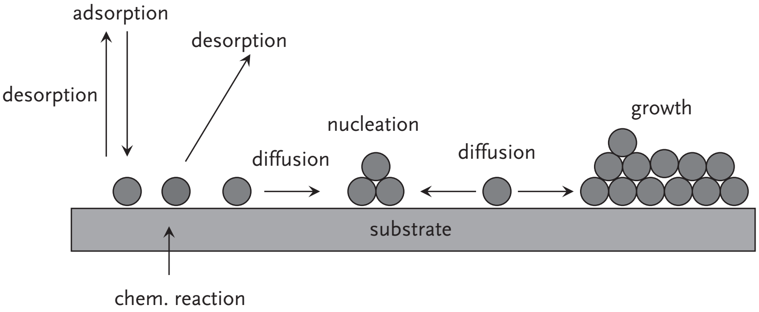

Figure 1.4 Schematic illustration of surface processes in thin film and nanostructure growth including adsorption–desorption, diffusion, nucleation, and growth.

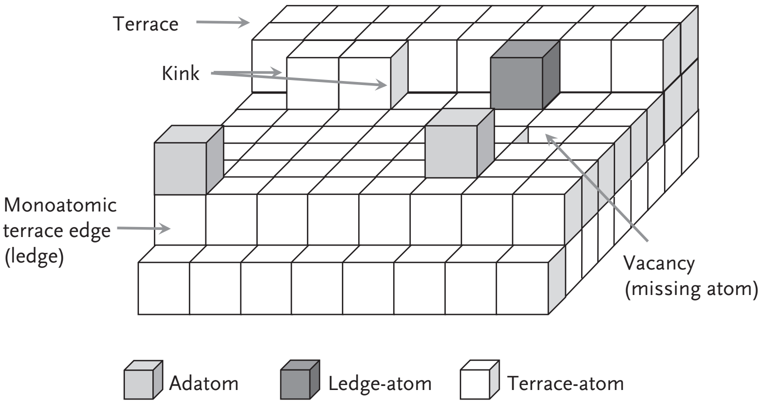

Figure 1.5 A model surface (TSK model) to illustrate the coordination number of different atomic bonding sites on a surface.

to reach a new equilibrium state. The asymmetry in the electron screening at the surface plane leads to a relaxation of the outermost atomic layers, and periodic modulation of the interatomic distances perpendicular to the plane of the surface, but leaves the in-plane atomic positions intact; the symmetry of the lattice plane is conserved. This relaxation is most often observed for metals, while covalently bonded materials usually undergo a so-called reconstruction, where the atomic positions within the plane of the surface are modified and deviate from those of the equivalent plane within the 3D solid. The surface reconstruction is treated thermodynamically and kinetically like the formation of a new phase, and several different reconstructions can co-exist on a single surface orientation. The surface reconstructions can offer unique templates with atomic-scale corrugation and highly selective attachment sites. The guided or templated self-assembly of nanostructures on reconstructed surfaces has been used extensively, and several examples are included in Chapters 3 and 4.

The growth of a nanostructure or thin film is initiated by the adsorption of ad-atoms as the first step. When looking at an adsorption process we often distinguish between physisorption and chemisorption. Physisorption is characterized by weak bonding between surface and adsorbate. In Figure 1.6 the interaction potential for a fairly common reaction, dissociative chemisorption, is shown as a function of distance. The molecule A_2 approaches the surface, is physisorbed, and enters the shallow physisorption well. The weak, physisorption interaction is due to van der Waals forces, which arise from the interaction between dipoles created by quantum mechanical fluctuations of the electron charge distribution. The interaction between the incoming adsorbate atom/molecule and the electrons of the solid can be described reasonably well as a harmonic oscillator, where the oscillator coordinate is the trajectory of the incoming atom

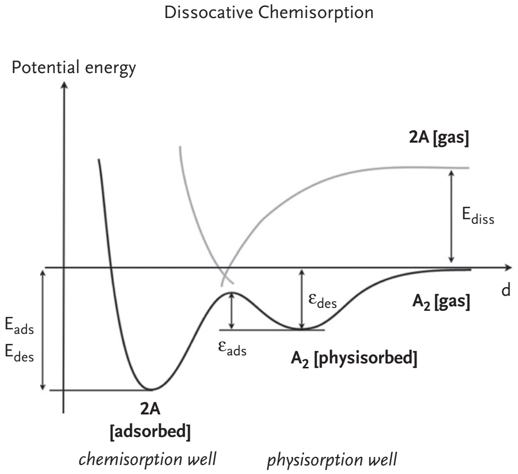

E_{diss} energy difference between [2A] atoms and the A_2 molecule

physisorption well

ε_{ads} energy barrier for dissociative adsorption

ε_{des} energy barrier for desorption

chemisorption well

E_{des} energy barrier for complete desorption

E_{ads} energy gain during to adsorption of atoms

Figure 1.6 Characteristic potential well of the relatively common dissociative chemisorption; the energy is shown as a function of the surface–ad-atom separation, and the origin of the energy axis is the potential energy of a molecule far away from the surface. A wider range of surface reactions and interaction potentials is discussed in [13].

normal to the surface [11]. The adsorption of noble gases at surfaces only shows a physisorption well, and the energy levels within that well agree closely with the simple harmonic oscillator model.

The repulsive term at shorter distances comes from the Pauli exclusion principle, due to the onset of overlap between the closed shell electrons in the atom and the electrons “spilling out” of the solid. The equilibrium distance of a physisorbed atom or molecule from the surface is relatively large, and about 0.3 nm above a noble metal surface for He [12]. The minimum in the potential well is shallow and the physisorption binding energy consequently relatively small. Energy levels within a physisorption well have been probed by scattering experiments. For comparison, the bond length for a covalent bond is only about 0.1–0.15 nm. Each atom or molecule approaching a surface will move through the physisorption potential well before the much stronger, short range chemisorption interaction begins to dominate, or the atom is ejected back into the vacuum. The ad-atom can only be captured in an adsorption well if it can reduce its kinetic energy sufficiently to occupy one of the energy states within the well. This relaxation is often achieved by electronic or vibrational excitation of the surface, which is then dissipated into the bulk. In the example for dissociative chemisorption the activation energy to the chemisorption well with two A atoms is lower than desorption into the vacuum or adsorption as a A_2. Dissociation is therefore the favored reaction pathway.

The chemical interaction of an adsorbate with a surface is considerably more complex than physisorption. A reasonable description of physisorption can be achieved by treating the surface as homogenous and featureless entity; however, the formation of a chemical bond is highly sensitive to the local geometric and electronic structure of the surface. A multitude of reaction scenarios is known, and have been investigated in great detail in the study of surface reactions of relevance in catalysis. The chemisorption process is particularly complex for molecules where the orientation of the molecule relative to the surface, the surface structure, and rotational and vibrational internal degrees of freedom within the molecule determine the reaction pathway. The reaction process between ad-atom and surface can be described by using a potential energy surface with two (three) coordinates: one (two) in the surface, and one for the distance between ad-atom and surface. This description captures the relative orientation of the ad-atom with respect to the surface, and includes the physi- and chemisorption wells.

An example of the interplay between adsorption and desorption processes in the synthesis of nanostructures is the formation of graphene sheets: one method uses the pyrolysis of hydrocarbon molecules on transition metal surfaces, and another frequently used approach employs desorption of silicon from a SiC surface, so that the graphene layer is left behind. These processes are described in detail in Chapter 6.

Adsorption and desorption processes are the initial steps in the synthesis of thin films and nanostructures, and the ad-atom bonding site is determined by the random selection of the initial impact site and the shape of the potential well as a function of position and ad-atom orientation. However, the initial bonding site might only present a local minimum in the potential energy surface. Probing of adjacent sites and motion into a lower energy position can only be accomplished by diffusion. Diffusion can happen on a very short length scale and just be perceived as a repositioning of the ad-atom, or it can involve transport on long length scales across a large section of the surface. The interplay between the kinetic aspects, such as diffusion, and the thermodynamic drive to minimize the energy of the system can be used to modulate nanostructure geometry over a very wide range. Diffusion of ad-atoms involves a multitude of different mechanisms on an atomic length scale, and a detailed discussion can be found in many surface science textbooks, such as Ref. [13]. We are concerned here mostly with the impact of diffusive and kinetic processes on the growth, morphology, and geometry of nanostructures.

The homoepitaxy of metal films is a particularly powerful example to illustrate the interplay between thermodynamic and kinetic control of surface processes. The homoepitaxy of several metals is very well studied and an extensive discussion is given in Ref. [14]. In thermodynamic equilibrium the deposition of Pt on a Pt surface should lead to a layer-by-layer growth; no strain is built up at the interface and a Pt overlayer perfectly wets a Pt surface [14–17]. However, the layer-by-layer growth and consequently formation of a smooth Pt overlayer is only observed at relatively high temperatures, which indicates the presence of energy barriers, which inhibit the movement of Pt ad-atoms into energetically favorable bonding sites. The deviation of the homoepitaxy of Pt on Pt from the layer-by-layer growth mode can only be explained by kinetic arguments, and the presence of an activation barrier of sufficient height to impede the adoption of the energetically most favorable layer structure. We will take a closer look at two of the wide range of structures which form in the homoepitaxial growth of Pt layers and are shown in Figure 1.7: the fractal structures, which form at relatively low temperatures and are most prominent at low coverages, and the pancake, or stacked, layer structure, whose formation requires an elevated temperature.

The fractal structure forms in a so-called "hit and stick" process: the Pt ad-atoms possess only limited mobility on the surface, and will become immobile once they bond with another highly unsaturated ad-atom. They cannot overcome the activation barrier for detachment from an energetically unfavorable position, and will "stick" at their initial attachment site after they "hit" another ad-atom or an unsaturated bond. Many fractal structures show a preferential orientation with respect to the underlying surface structure, which is an indication of preferential, easier directions of

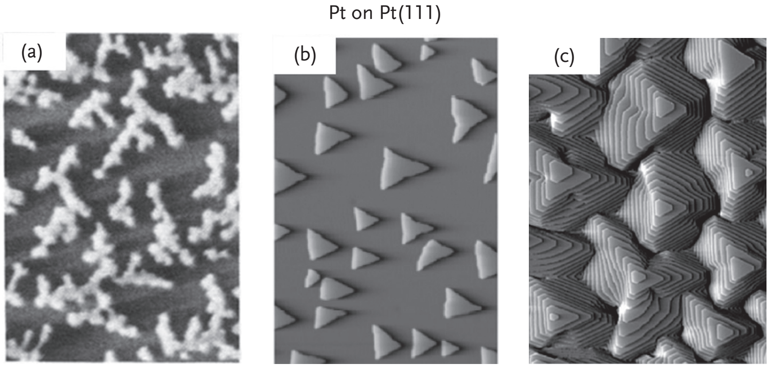

deposition rate: $1{\cdot}10^{-3}$ ML/s
temperature: 200 K
coverage: 0.2 ML Pt

deposition rate: $1{\cdot}10^{-3}$ ML/s
temperature: 400 K
coverage: 0.2 ML Pt

deposition rate: $7{\cdot}10^{-3}$ ML/s
temperature: 440 K
coverage: 12 ML Pt

Figure 1.7 The growth of fractal and compact island structures can be observed in the homoepitaxy of Pt on the Pt(111) surface [15–17]. The structural variability is controlled by a hierarchy of activation barriers. The critical processing parameters are deposition rate, temperature, and coverage and they control structure formation during homoepitaxial growth on a clean sample. The presence of traces of some adsorbates such as CO can alter the activation barriers decisively and push the system into a different growth mode. Fig. 1.7(a) and (b) reprinted with permission from [15] and [16] . Copyright (1998 and 1993, respectively) by the American Physical Society. Fig. 1.7 (c) is reprinted from [17] with permission from Elsevier.

diffusion (diminished activation barrier for diffusion) or detachment. Fractal structures have also been observed for fullerene islands on a fullerene surface [18, 19], and are present in many low temperature processes. If the temperature is increased many of the ad-atoms, which are initially positioned in unfavorable bonding sites can now reposition themselves and probe a multitude of sites.

The critical barrier for ad-atom motion, which leads to the formation of stacked structures, is the Ehrlich–Schwöbel barrier [20, 21]. This is the additional energy required for motion of an ad-atom across a step edge from the higher to the lower terrace compared with the activation barrier to move on the terrace. The origin of the additional barrier is a rearrangement in the spatial distribution of electrons around a highly unsaturated step edge atoms. Any ad-atom landing on the upper level of a terrace is now trapped on that terrace, and will be repulsed from the step edge. The distance between step edge and the boundary of the new island on the upper level corresponds to the diffusion length of the ad-atom. The magnitude of the Ehrlich–Schwöbel barrier is strongly system and material dependent. Once the temperature is sufficiently high, and ad-atoms can overcome this activation barrier, the layer-by-layer growth, which is predicted based on solely thermodynamic arguments, will proceed. The interplay between a multitude of activation barriers is key to achieving a deterministic approach in nanostructure fabrication, and a kinetic description based on the individual reaction rates for the atomistic processes has to be used for a full comprehension of growth far from equilibrium.

The next step in the growth of layers, wires, and nanostructures is the formation of a stable nucleus, which then proceeds to grow by further accumulation of ad-atoms. Classic nucleation theory as described in many textbooks has many limitations, but it is used here to illustrate the role of the surface energy during the initial nucleation phase of a seed crystal. The condensation of the solid seed crystal is driven by the change in Gibbs free energy with nucleus size – the total change in Gibbs free energy is the sum of bulk, surface and interface contributions. The contributions to the change in Gibbs free energy as a function of nucleus radius r are a volume component given by:

$$\Delta G_{\mathrm{bulk}} = \frac{4}{3}\pi\rho r^3 \Delta\boldsymbol{\mu}_{s,l} \tag{1.9}$$

and a surface contribution

$$\Delta G_{\mathrm{surface}} = 4\pi r^2 \gamma_{s,l} \tag{1.10}$$

where ρ is the density of the solid, $\Delta\mu_{\mathrm{s,l}}$ is the chemical potential difference, and $\Delta\gamma_{\mathrm{s,l}}$ is the interfacial energy at the solid–liquid *s,l* interface. The surface contribution to the Gibbs free energy dominates for small particles prior to reaching the critical nucleus size, and can indeed drive the formation of a phase, which is surface stabilized and does not represent the most stable bulk structure. At larger particle sizes, the bulk contribution becomes decisive due to its r^3 dependence on the particle radius. The surface-stabilized nucleus will only survive if the energy difference between the competing phases is relatively small, which is indeed the case for many of nanowires made of compound semiconductors considered in Chapter 3.

1.3
Closing Remarks

Confinement and dimensionality are concepts which are at the center of nanoscience and technology and will accompany us throughout this book. A nanoscale structure and material is defined with these concepts in mind, and they are the driving force for the rapid and often astonishing modification of properties as a function of diminishing size. In this book we mostly focus on electronic, and in some instances optical and chemical, properties of nanoscale materials, and confinement is therefore defined in terms of characteristic length scales inherent in the electronic structure, such as de Broglie wavelength.